JOURNAL OF NUCLEAR MATERIALS 18 (1966) 39–54. © NORTH-HOLLAND PUBLISHING CO., AMSTERDAM

TEMPERATURE DEPENDENCE OF THE ELASTIC MODULI IN ALPHA URANIUM SINGLE CRYSTALS, PART IV (298° to 923° K)

E. S. FISHER

Metallurgy Division, Argonne National Laboratory, Argonne, Illinois, USA

Received 14 May 1965

The single crystal elastic moduli for alpha uranium have been measured as a function of temperature between 298° and 923° K. These data, together with those previously reported, permit a description of the elastic properties of uranium at temperatures from 42° K to 12° K below the $\alpha \rightarrow \beta$ phase transformation. Abnormal changes in the temperature dependence of certain shear and Young's moduli occur above 350° K. It is shown that the changes in temperature dependence of the elastic properties are probably responsible for the contraction of b_0 lattice constant with increasing temperature and are reflected in the anomalous increase in the lattice specific heat above 350° K. It is suggested that the anomalies and the marked decrease in temperature dependence of the electrical resistivity above 400° K are associated with a gradual disappearance of magnetic ordering.

Les modules élastiques de monocristaux d'uranium α ont été mesurés en fonction de la température entre 298° et 923° K. Ces données, ainsi que celles reportées dans la littérature, permettent de se représenter les propriétés élastiques de l'uranium aux températures comprises entre 42° K et 12° K en dessous de la température de transformation $\alpha \rightarrow \beta$. Des variations anormales dans la relation entre température et modules de cisaillement et modules d'Young se produisent au-dessus de 350° K. On a montré que ces variations dans les propriétés élastiques en fonction de la température sont probablement responsables de la contraction du paramètre réticulaire b_0 avec la température croissante et ces variations anormales sont responsables aussi de l'accroissement anormal de la chaleur spécifique réticulaire au-dessus de 350° K. Il est suggéré que les anomalies et la diminution marquée dans la variation de la résistivité électrique en fonction de la température au-dessus de 400° K sont associées à une disparition progressive de l'ordonnancement magnétique.

Es wurde der Elastizitätsmodul für α-Uran an Einkristallen im Temperaturbereich von 298° K bis 923° K gemessen. Diese Daten erlauben im Zusammenhang mit früher veröffentlichten Zahlen eine Beschreibung der elastischen Eigenschaften von Uran bei Temperaturen von 42° bis 12° K unterhalb der α-β-Phasenumwandlung. Ein abnormaler Wechsel in der Temperaturabhängigkeit des Schermoduls und von Young's Modul kommt im Bereich von 350° K vor. Es konnte gezeigt werden, dass die Änderungen in der Temperaturabhängigkeit der elastischen Eigenschaften wahrscheinlich verantwortlich sind für die Kontraktion des Gitterparameters b_0 mit ansteigender Temperatur. Sie finden ihren Ausdruck im anomalen Anstieg der spezifischen Wärme oberhalb 350° K. Es wird angenommen, dass die Anomalien und der bemerkenswerte Abfall in der Temperaturabhängigkeit des elektrischen Widerstandes oberhalb 400° K mit dem stufenweisen Verschwinden einer magnetischen Ordnung in Zusammenhang stehen.

1. Introduction

This paper presents the results of a fourth series of measurements which are part of a program originally intended to determine the elastic properties of alpha uranium single crystals in the temperature range of 4° to 935° K, the latter being the temperature of the $\alpha \rightarrow \beta$ structural transformation. For orthorhombic symmetry there are nine principal elastic moduli needed to describe the elastic properties. The measurements at 298° K and the temperature dependence of all of the moduli in the range of 42° K to 298° K are reported in [1–3]), the latter reference giving very clear

† This work was performed under the auspices of the United States Atomic Energy Commission.

evidence of a nonstructural phase transition at 42° ± 1° K. Several attempts to measure all of the elastic moduli between 4° and 42° K have been unsuccessful because of very large acoustic attenuation for the majority of the ultrasonic wave modes; some data in the 4° to 42° K range are however, given in [3]).

In addition to a complete set of results covering the 78° to 298° K range, ref. [2]) contains the temperature dependence of the principal compressional moduli, c_{11}, c_{22} and c_{33}, up to 573° K. To complete the data between 298° and 935° K it was necessary to experiment with various coupling media and to develop techniques appropriate for the propagation of both longitudinal and transverse ultrasonic waves in small single crystals at temperatures considerable above ambient in vacuum.

The incentive to complete the studies in this temperature range arose from several areas of interest. First, the linear compressibility in the [100] direction has a negative temperature dependence in the range of 42° to 298° K. This anomaly together with some neutron diffraction results of Mueller *et al.* indicate that some type of magnetic order may exist in alpha uranium at temperatures above 298° K [4]). Secondly, at temperatures above 298° K there are several anomalies in other properties of alpha uranium, including a negative thermal expansion in the [010] direction [5]), the temperature dependence of the electrical resistance [6]) and specific heat [7]) and a severe temperature dependence of the critical resolved shear stress for (001) [100] slip as a plastic deformation mechanism [8]). Friedel [9]) has suggested that the thermal expansion and specific heat anomalies are the result of thermally excited changes in the electronic band structure which cause a rupture of the strong binding between the two nearest neighbor bonds and a corresponding increased attraction between third and fourth nearest neighbors, the latter leading to an increase with temperature of the vibrational frequency for certain thermal modes and a consequent negative curvature in electrical resistance versus temperature curve. In the cases of hcp titanium and zirconium such negative curvatures correspond closely to pronounced positive curvatures in certain shear modulus versus temperature curves [10]).

2. Experimental procedures

2.1. Sample preparation

Eight different single crystal plates and six different crystal orientations relative to the plate faces were used in this study. The preparation, physical dimensions and orientations of the plates are given in [1, 2]). The samples ranged in thickness from 2 to 3 mm with lateral dimensions of 4 to 6 mm.

2.2. Measuring technique

The measurement of the change in ultrasonic wave velocity with temperature for each of the three wave modes possible to propagate in each of six different crystal directions was carried out using the phase comparison technique described in [2]). The basic equation is as follows:

$$\frac{V}{V_0} = \frac{t}{t_0} \cdot \frac{f_n}{(f_n)_0} \left[\frac{n + \gamma_0/2\pi}{n + \gamma/2\pi} \right], \qquad (1)$$

where V is the wave velocity to be determined at any given temperature relative to a reference velocity V_0, which is that, measured at 298° K. The wave frequency $(f_n)_0$ corresponds to n integral wave lengths in a sample thickness of $2\ t_0$ for a velocity V_0 at 298° K. Disregarding the quantities in square brackets, V at any given temperature can be obtained from a measurement of f_n corresponding to the same number of wave lengths, n, as were present at 298° K and from a calculation of t, the specimen thickness at that temperature, using existing thermal expansion data. The quantity in square brackets arises from the change in the phase angle γ with temperature, $\gamma/2\pi$ being the correction to n necessary to account for the phase shift within the coupling material. The evaluation of γ has been described by McSkimin [11]). In the present measurements this correction was neglected in view of the very small $\gamma/2\pi$ values estimated from the relative intensities of the reflected wave trains.

2.3. Measuring apparatus

With exception for the coupling cement, the apparatus used for the measurements was precisely the same as described in [10]) for measurements above 300° K. The sample was separated vertically from the piezoelectric transducer by a 20 to 25 mm long fused silica buffer rod. A very thin layer of phenolic resin paste, described in [12]), was used to couple the sample acoustically to the buffer rod. Contrary to the information given in [12]), the present experiments have shown that this cement can propagate both longitudinal and transverse waves up to temperatures of 923° to 933° K.

The measurements of f_n were carried out in the range of 35 to 45 mc/sec for both types of waves. The recorded temperatures were obtained from a chromel-alumel thermocouple with the hot junction located about 3 to 4 mm from the specimen but in contact with the fused silica buffer. Since errors of 2° or 3° K were possible because of natural thermal gradients in the heated zone and fluctuations in the controlling temperatures it was deemed advisable to limit the temperatures of measurement to 928° K, so as to insure against destroying the single crystal character of the samples by the $\alpha \rightleftarrows \beta$ transformation. In the early stages

Table 1

Temperature ranges at which attenuation of ultrasonic waves prevented measurement of wave velocities
ϱ = density V = wave velocity

Crystal Designation	Direction of wave propagation	Type of mode and shear polarization	Stiffness modulus	Temperature ranges of missing data, (° K)
A, A′	100	Long.	c_{11}	
		Shear, [010]	c_{66}	above 325
		Shear, [001]	c_{55}	600–825
B, B′	010	Long.	c_{22}	580–650, above 850
		Shear, [100]	c_{66}	above 340
		Shear, [001]	c_{44}	above 375
C	001	Long.	c_{33}	
		Shear, [010]	c_{44}	very weak (825–835)
		Shear, [100]	c_{55}	above 825
D	$\theta_T \sim 45.5°$ to [001], 90° to [010]	Quasi-long.	ϱV^2_{D}	above 750
		Quasi-shear, [$h0l$]	$\varrho V^2_{\mathrm{DS}}$	
		Pure shear, [010]	$\varrho V^2_{\mathrm{DPS}}$	
E	$\theta_{\mathrm{E}} \sim 38°$ to [001], 90° to [100]	Quasi-long.	ϱV^2_{E}	
		Quasi-shear, [0kl]	$\varrho V^2_{\mathrm{ES}}$	
		Pure-shear, [100]	$\varrho V^2_{\mathrm{EPS}}$	above 300 above 300
F	$\theta_{\mathrm{F}} \sim 44.5°$ to [100], 90° to [001]	Quasi-long.	ϱV^2_{F}	
		Quasi-shear, [hk0]	$\varrho V^2_{\mathrm{FS}}$	740–860
		Pure-shear, [001]	$\varrho V^2_{\mathrm{FPS}}$	700–823

of the study one of the crystals was intentionally heated to 935° K to test the possibility that either the transformation temperature may be higher than 935° K with single crystals and/or that the transformation does not destroy the sample, as is the case for titanium and zirconium [10]). After cooling, this crystal was polycrystalline and physically deformed, indicating that neither of the above suppositions is correct.

2.4. Limitations caused by attenuation

A complete set of data for determining all nine elastic stiffness moduli and the available cross checks, or internal consistency tests, at all temperatures required that the velocities of 18 different wave modes be measured at intervals of 10° to 20° between 298° K and 923° K. In fact, however, this schedule was not accomplished primarily because of acoustic energy losses within the uranium samples. These losses occurred for a majority of wave modes within temperature regions which varied in range and limits and did not appear significantly affected by frequency changes within the range of 30 mc/sec to 50 mc/sec. The losses were encountered in all samples, but only for certain wave modes and they occurred in reproducible temperature ranges during successive attempts to complete the measurements. In addition to these sample losses there occurred temperature and frequency dependent background losses caused by scattering of the acoustic waves within the buffer rods; consequently, it was not possible to measure the magnitude of the losses within the samples. The temperature ranges in which these losses prevented continuous measurements are given in table 1. The difficulties in measuring the shear mode velocities in crystal E above 300° K were apparently caused by a deformation kink produced during refacing the crystal after low temperature measurements were completed. The causes for the high attenuation above 325° K for both shear modes

Table 2

Equations used for evaluation of stiffness moduli

Modulus	Equation	Temperature range (°K)
c_{11}	Direct	298–923
c_{22}	(1) Direct	298–580, 650–850
	(2) $\dfrac{\varrho V^2_F+\varrho V^2_{FS}-c_{11}^2\cos^2\theta_F-c_{66}}{\sin^2\theta_D}$	298–740, 860–923
c_{33}	Direct	298–923
c_{44}	(1) Direct, B	298–375
	(2) Direct, C	298–923
c_{55}	(1) Direct, A	298–600, 825-923
	(2) Direct, C	298–825
	(3) $\dfrac{\varrho V^2_F-c_{44}\sin^2\theta_F}{\cos^2\theta_F}$	298–700, 823–923
	(4) $\varrho V^2_D+\varrho V^2_{DS}-c_{33}\cos^2\theta_D-c_{11}\sin^2\theta_D$	298–750
c_{66}	(1) Direct, B	298–340
	(2) $\dfrac{\varrho V^2_{DPS}-c_{44}\cos^2\theta_D}{\sin^2\theta_D}$	298–923
	(3) $\varrho V^2_{FL}+\varrho V^2_{FS}-c_{11}\cos^2\theta_F-c_{22}\sin^2\theta_F$	298–580, 650–740, 860–923, from extrapolated c_{22}
c_{12}	(1) $f(\varrho V^2_F, c_{11}, c_{22}, c_{66})$	298–923
	(2) $f(\varrho V^2_{FS}, c_{11}, c_{22}, c_{66})$	298–740, 860–923
c_{13}	(1) $f(\varrho V^2_D, c_{11}, c_{33}, c_{55})$	298–750
	(2) $f(\varrho V^2_{DS}, c_{11}, c_{33}, c_{55})$	298–923
c_{23}	$f(\varrho V^2_E, c_{33}, c_{22}, c_{44})$	298–923

propagated in the [010] direction, the c_{66} shear mode in crystals A and A' and the c_{44} shear mode may be related to the twinning dislocations present in all the crystals. The occurrence of thin [130] type twins during the crystal growth process is very difficult to prevent. The occurrence of high attenuation in intermediate temperature regions only, however, seems to be associated with certain features in the temperature dependence of certain elastic moduli and the correspondence is noted in the discussion to this paper.

With exception for the [010] direction, there was at least one mode for each direction of propagation for which velocity measurements could be made over the full temperature range, thus permitting direct evaluation of c_{11}, c_{33}, c_{44}, ϱV^2_{DS}, ϱV^2_{EL} and ϱV^2_{FL}. The equations used for evaluating each of the nine stiffness moduli are given in table 2. The c_{22} modulus was evaluated directly over most of the temperature range and was derived from indirect data, involving five different wave modes, in those ranges where direct data were missing. In addition, cross-checks were available over most of the temperature range. The c_{55} shear modulus was derived directly over the whole range by combining the measurements from crystals A and C. Cross-checks for c_{55} were available over most of the range. Since direct measurements of c_{66} were missing above 340° K, it was necessary to resort to two different sets of indirect measurements to complete the data for this modulus. Cross-checks between the indirect measurements of c_{66} were available over a 450° K range.

Once the diagonal moduli, $c_{11} \ldots c_{66}$, were evaluated the cross coupling moduli, c_{12}, c_{13} and c_{23} were computed using the equations given in sec. 4.4 of [2]). These moduli are derived from the measured ϱV^2 of either the quasi-longitudinal or quasi-transverse modes of crystals D, E and F. For c_{12} and c_{13} the quasi-transverse mode velocities were used because of smaller errors introduced to the computations of the moduli, as described in [1]).

3. Results

3.1. External checks

A comparison of the present c_{11}, c_{22} and c_{33} measurements with those reported in [2]) for the temperature range 298° to 573° K offers a direct check on the treatment of the present data and the technique of temperature measurement, since those [2]) data were obtained using a silicone oil coupling and a silicone oil bath as a heating medium. Fig. 1 shows the basic data, $f_n/(f_n)_0$ of eq. (1), for the two sets of measurements in the 298° to 573° K temperature range. The data for c_{11} and c_{22} using the present arrangement show no significant disagreement with the previous data, thereby, confirming that the bracketed terms in eq. (1) could be neglected without introducing errors greater than 0.05 % in the basic data. The data for c_{33} do, however, show significant disagreements, especially in the range of 400° to 500° K where the difference

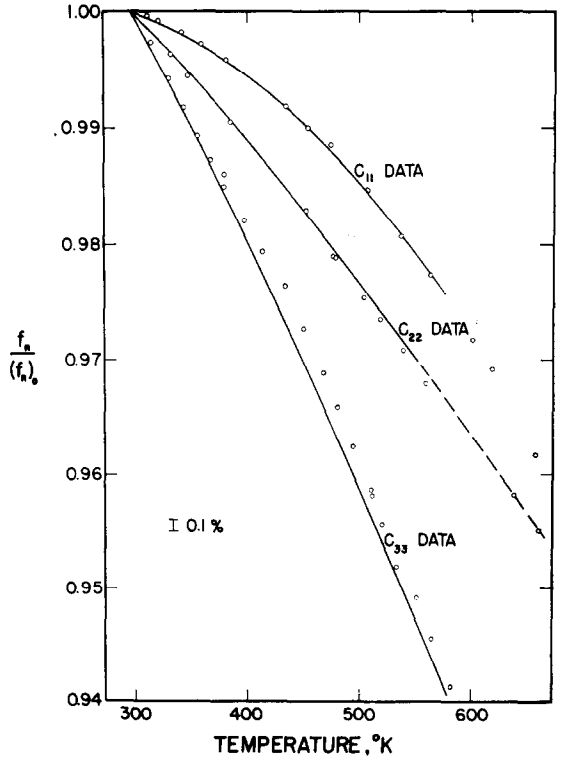

Fig. 1. Comparison of data obtained by present technique (o), with data obtained in silicone oil bath (——), ref. [2]).

reaches a maximum of 0.3 %. The points for the present data shown in the figure represent two different runs; it is, consequently, difficult to ascribe these differences to temperature gradients between the sample and the thermocouple. There is, therefore, no apparent explanation; nevertheless, the differences diminish to approximately 0.15 % in the range of 500° to 573° K and a line through the present data gives a slope corresponding to that of previous data above 500° K. It may then be assumed that no serious errors exist in the present data above 573° K.

3.2. Internal consistency of data

As indicated in table 2, the data obtained provide several means of computing c_{22}, c_{55} and c_{66}. The curves obtained using the different equations of table 2 are compared in fig. 2, where the values of the three moduli, normalized to the 298° K values, are plotted over the range from 298° to 923° K. For c_{55}, the values computed directly from the crystal A data are in exceptionally good agreement with those computed from eq. c_{55} (4) between 298° and 600° K. The latter equation gives c_{55} up to 750° K and the c_{55} (1) data are again available above 825° K. The curve drawn through these two sets of c_{55} values and the c_{55} values below 298° K, given in [2]), has two linear parts, one extending from 250° to about 425° K and the other between 450° to 923° K with a relatively sharp curvature between 425° and 450° K. The c_{55} values from crystal C and eq. c_{55} (3), however, deviate positively from this curve by a maximum of 0.8 % at 450° K and give slightly lower values in the 800° to 900° K range. Although the deviations are relatively minor, a curve constructed using the latter two sets of data would not blend into the low temperature data using a linear plot and would indicate a positive curvature in the 700° to 800° K range.

For c_{66}, the few data points obtained from crystal B and the values from eq. c_{66} (3) blend in smoothly with the low temperature measurements and are in remarkably good agreement with the eq. c_{66} (2) points up to 740° K. Furthermore, by assuming a smooth curve for the

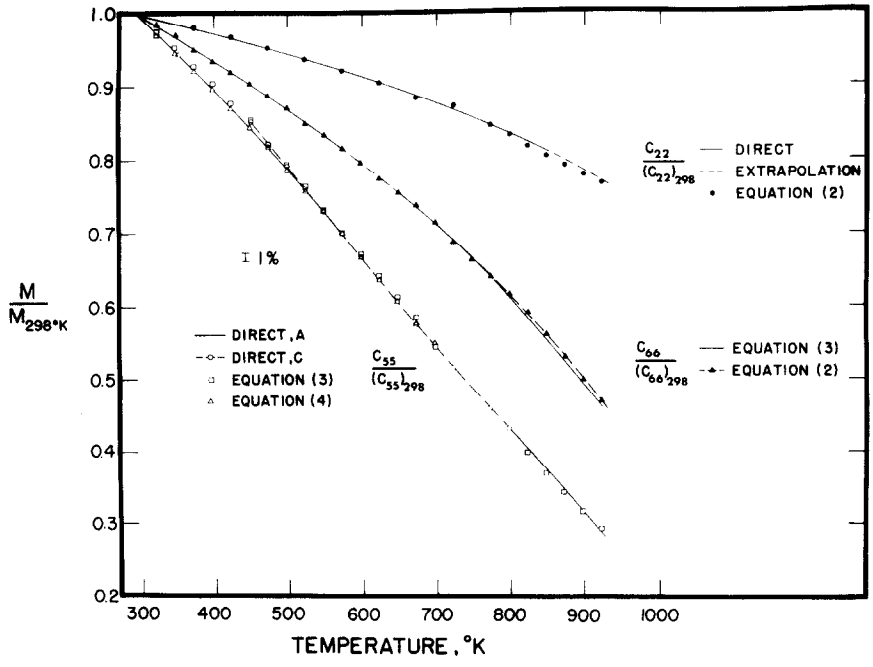

Fig. 2. Comparison of the normalized modulus values for c_{22}, c_{66} and c_{55} as evaluated from different sets of data using equations given in table 2.

ϱV^2_{FS} vs temperature plot, the interpolated values of ϱV^2_{FS} between 740° and 800° K used in eq. c_{66} (3) give c_{66} values which are in good agreement with eq. c_{66} (2). Between 800° and 850° K, however, the eq. c_{66} (2) values are significantly higher with deviations as great as 1 %. To decide the question of which are the more probably correct values, eq. c_{66} (3) can be restated so as to compute c_{22} indirectly using one or the other c_{66} values, i.e. eq. c_{22} (2). As shown in fig. 2, the c_{22} computed from eq. c_{66} (2) fall about 0.8 % lower than the directly measured c_{22} between 800° and 850° K and indicate an unlikely step in the c_{22} vs temperature curve. As in the adjudication of c_{55}, we dismiss the 0.8 % deviation as due to unknown origin

TABLE 3

Elastic stiffness moduli for α-U at various temperatures between 44° and 923 °K (10^{12} dyn/cm²)

Temp. (°K)	c_{11}	c_{22}	c_{33}	c_{44}	c_{55}	c_{66}	c_{12}	c_{13}	c_{23}
44	1.500	2.085	2.868	1.407	0.892	0.849	0.275	0.345	1.123
46	1.610	2.090	2.875	1.411	0.901	0.851	0.294	0.320	1.118
48	1.685	2.093	2.878	1.412	0.905	0.851	0.318	0.305	1.115
50	1.740	2.094	2.879	1.411	0.906	0.851	0.339	0.292	1.112
60	1.900	2.095	2.879	1.407	0.904	0.848	0.388	0.256	1.106
73	1.993	2.093	2.875	1.400	0.896	0.844	0.403	0.239	1.098
98	2.063	2.081	2.856	1.384	0.879	0.833	0.425	0.226	1.098
123	2.103	2.070	2.835	1.367	0.862	0.822	0.430	0.221	1.097
148	2.125	2.058	2.813	1.349	0.844	0.811	0.435	0.218	1.095
173	2.138	2.046	2.791	1.332	0.826	0.799	0.441	0.216	1.091
198	2.145	2.035	2.768	1.314	0.807	0.788	0.446	0.216	1.088
223	2.149	2.023	2.745	1.297	0.789	0.777	0.451	0.216	1.084
248	2.151	2.011	2.721	1.280	0.771	0.766	0.454	0.216	1.081
273	2.151	1.998	2.696	1.262	0.753	0.754	0.458	0.216	1.078
298	2.148	1.986	2.671	1.244	0.734	0.743	0.465	0.218	1.076
323	2.144	1.973	2.647	1.228	0.715	0.731	0.471	0.220	1.074
348	2.139	1.961	2.623	1.210	0.695	0.718	0.476	0.222	1.070
373	2.132	1.947	2 597	1.193	0.677	0.708	0.479	0.223	1.069
398	2.125	1.934	2.571	1.176	0.659	0.696	0.483	0.226	1.064
423	2.117	1.919	2.543	1.158	0.640	0.686	0.485	0.228	1.058
448	2.107	1.904	2.513	1.141	0.620	0.675	0.488	0.230	1.052
473	2.097	1.889	2.485	1.122	0.601	0.661	0.494	0.235	1.044
498	2.087	1.874	2.456	1.104	0.579	0.648	0.501	0.240	1.034
523	2.076	1.859	2.427	1.084	0.557	0.632	0.506	0.245	1.027
548	2.063	1.843	2.398	1.065	0.535	0.620	0.511	0.250	1.018
573	2.049	1.827	2.369	1.045	0.513	0.607	0.517	0.257	1.009
598	2.034	1.811	2.338	1.024	0.491	0.591	0.523	0.263	1.000
623	2.018	1.794	2.309	1.003	0.469	0.576	0.528	0.270	0.994
648	2.002	1.777	2.278	0.981	0.448	0.562	0.533	0.276	0.991
673	1.984	1.760	2.249	0.958	0.426	0.546	0.537	0.282	0.987
698	1.965	1.743	2.219	0.937	0.404	0.531	0.540	0.288	0.984
723	1.946	1.724	2.187	0.916	0.383	0.515	0.543	0.297	0.981
748	1.925	1.703	2.153	0.895	0.361	0.497	0.552	0.304	0.976
773	1.904	1.681	2.118	0.873	0.340	0.477	0.566	0.312	0.971
798	1.882	1.658	2.082	0.850	0.318	0.456	0.578	0.320	0.969
823	1.858	1.635	2.049	0.826	0.295	0.433	0.592	0.328	0.967
848	1.832	1.610	2.013	0.804	0.273	0.411	0.603	0.338	0.962
873	1.804	1.584	1.977	0.780	0.253	0.388	0.612	0.349	0.959
898	1.775	1.562	1.942	0.757	0.232	0.365	0.624	0.361	0.954
923	1.742	1.535	1.907	0.734	0.211	0.344	0.630	0.374	0.953

and prefer to extrapolate the c_{22} values beyond the directly measured upper limit (850° K) assuming a smooth curve, which is parallel to that obtained from the spurious values. When these extrapolated c_{22} values are used in eq. c_{66} (3), the c_{66} values up to 923° K fall along a linear extrapolation of 298° to 850° K curve. With regard to the shape of the c_{66} vs temperature curve, both equations show the same abnormally large curvatures, between 500° and 800° K.

If 0.5 % probable error at 923° K is assumed for each of the diagonal moduli and the ϱV^2 values, the largest probable errors in c_{12}, c_{13} and c_{23} are 1.5 %, 3 % and 1 % respectively.

3.3. Temperature dependence of the stiffness moduli

Values of the nine stiffness moduli at temperatures between 44° and 923° K are given in table 3. The smoothed curves for c_{11}, c_{22} and c_{33} are given in fig. 3 along with those for ϱV^2, ϱV_E^2 and ϱV_F^2. [The c_{11} curve below 44° K is shown in [3])]. Between 298° and 923° K the curves have increasing negative curvatures. The temperature coefficients $(1(c_{ii})/(\mathrm{d}c_{ii}/\mathrm{d}T)$, decrease from −57 ppm/°K at 298° K to −640 ppm/°K at 923° K for c_{11}, from −251 ppm/°K at 298° K to −630 ppm/°K at 923° K for c_{22} and from −280 ppm/°K to −718 ppm/°K for c_{33}.

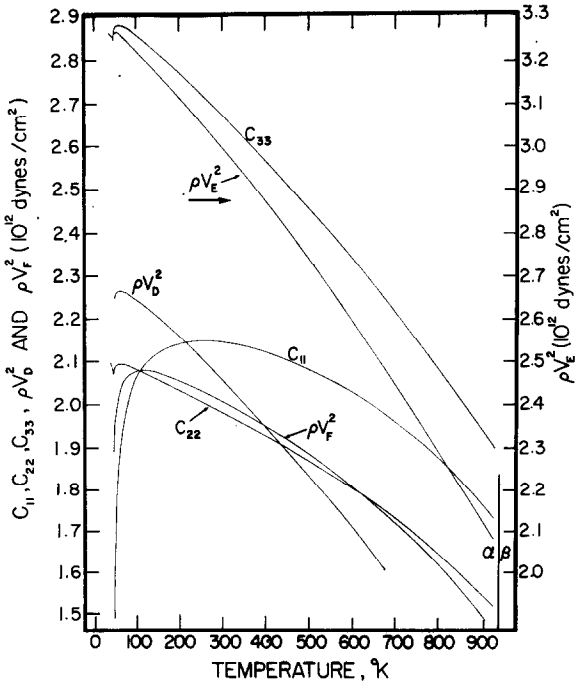

Fig. 3. Temperature dependence of the compressional stiffness moduli for alpha uranium.

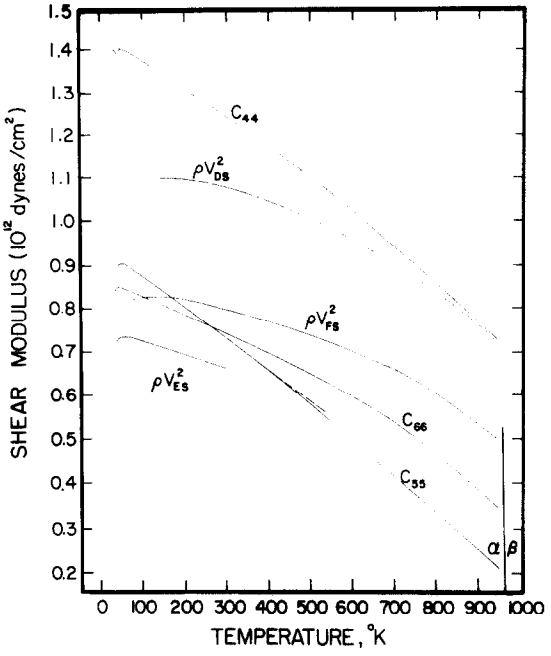

Fig. 4. Temperature dependence of the shear stiffness moduli for alpha uranium.

The smoothed curves for the shear moduli are shown in fig. 4. These curves exhibit relatively abrupt changes in slope, in contrast to those for the compressional moduli. The c_{44} curve is very nearly linear between 200° and 500° K and again between 750° and 923° K. The temperature coefficients for c_{44} decrease from −560 ppm/°K to −1180 ppm/°K between 298° and 923° K. The c_{55} curve also consists of two very nearly linear parts, as described above, with significant curvature only between 425° and 450° K. The c_{55} temperature coefficients decrease from −1060 ppm/°K at 298° K to −3400 ppm/°K at 923° K. The c_{66} curve also consists of two linear parts, 200° to 400° K and 800° to 923° K; the curvature, however, is most pronounced in the 700° to 800° K range. At 298° K and 923° K the temperature coefficients

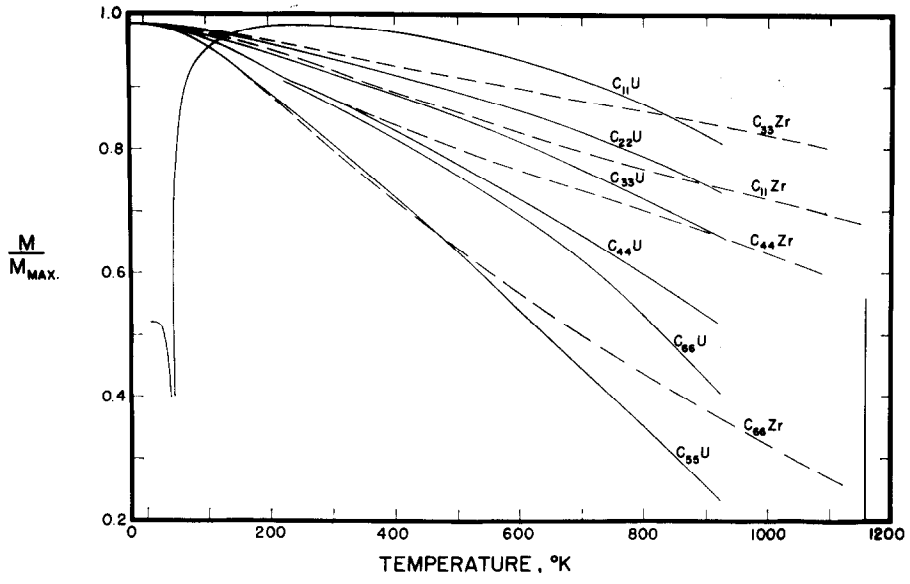

Fig. 5. Comparison of the temperature dependence of the principal stiffness moduli for alpha uranium and alpha zirconium [10]. Ordinate is the ratio of the modulus at temperature with respect to the maximum value of the modulus.

for c_{66} are -623 ppm/°K and -2300 ppm/°K respectively.

A comparison of the fractional change in the stiffness moduli with temperature is given in fig. 5, where the moduli are plotted as normalized to the respective maximum values. Included in the figure are the curves of the normalized moduli of zirconium [10]. Between 50° and 500° K the fractional change with temperature for c_{55} follows the c_{66} curve for zirconium very closely. The c_{66} zirconium curve, however, has a pronounced upward curvature, whereas c_{55} continues to decrease linearly with temperature to about 23 % of its maximum value. Similarly, c_{44} uranium follows the c_{44} zirconium curve very closely below 320° K but the differences increase at higher temperatures because of curvatures with opposite signs.

The c_{33} modulus for uranium undergoes the greatest decrease of the three principal compressional moduli. The total decrease in c_{33} from 50° K to 923° K is 34 %, compared to 27 % for c_{22} uranium and c_{11} zirconium. The c_{11} uranium decrease from the maximum value at 250° K is only 19 %.

The curves obtained from the c_{12}, c_{13} and c_{23} moduli, given in table 3, are shown in fig. 6. The c_{13} values give a relatively smooth curve, with a broad minimum between 175° and 275° K. The c_{12} values indicate a relatively sharp change in slope in the range of 725° K. In contrast to c_{12} and c_{13}, c_{23} decreases with increasing temperature.

3.4. Parameters computed from compliance moduli

Several informative aspects of this study appear in the temperature dependence of various combinations of the compliance moduli, which are computed from the inverse matrix of the stiffness moduli. The linear compressibilities,

$$\begin{aligned} \beta_{100} &= s_{11} + s_{12} + s_{13} \\ \beta_{010} &= s_{22} + s_{12} + s_{23} \\ \beta_{001} &= s_{33} + s_{13} + s_{23} \end{aligned} \qquad (2)$$

and the volume compressibility,

$$\beta_V = \beta_{100} + \beta_{010} + \beta_{001}$$

at various temperatures are given in table 4 and plotted in fig. 6. Upon heating from the phase transition at 41° K, β_{100} and β_{010} become

relatively insensitive to temperature in the range of 100° to 923° K. β_{100} decreases to a broad minimum between 200° and 600° K and increases by about 5 % before the α-β transformation. β_{010} shows a very small but continuous increase from 100° to 700° K and no significant change between 700° and 923° K. In contrast, β_{001} increases by 50 % between 70° and 923° K with an almost linear temperature dependence up to 400° K and a positive curvature above 400° K. At 923° K, β_{001} and β_{010} have about the same value, with β_{100} being about 30 % greater. The β_V values reflect primarily the β_{001} changes above 200° K.

TABLE 4

Young's moduli and compressibility parameters for α-U at various temperature between 440° and 923° K

	(10^{12} dyn/cm^2)			10^{-12} cm^2/dyn			
Temp. (°K)	E_{100}	E_{010}	E_{001}	β_{100}	β_{010}	β_{001}	β_V
44	1.447	1.632	2.236	0.572	0.321	0.154	1.048
46	1.557	1.637	2.261	0.531	0.315	0.166	1.012
48	1.629	1.637	2.273	0.504	0.308	0.175	0.987
50	1.680	1.635	2.281	0.485	0.303	0.181	0.969
60	1.827	1.626	2.294	0.440	0.293	0.196	0.929
73	1.915	1.625	2.299	0.419	0.291	0.202	0.912
98	1.977	1.604	2.277	0.402	0.290	0.207	0.899
123	2.013	1.588	2.253	0.394	0.290	0.210	0.894
148	2.033	1.574	2.231	0.389	0.291	0.212	0.892
173	2.043	1.560	2.209	0.386	0.291	0.215	0.892
198	2.047	1.546	2.187	0.384	0.291	0.217	0.892
223	2.048	1.532	2.164	0.382	0.292	0.219	0.893
248	2.048	1.518	2.139	0.381	0.292	0.221	0.895
273	2.045	1.502	2.114	0.380	0.293	0.223	0.896
298	2.037	1.486	2.088	0.380	0.293	0.226	0.899
323	2.033	1.470	2.062	0.379	0.293	0.228	0.899
348	2.024	1.455	2.038	0.378	0.293	0.230	0.901
373	2.014	1.437	2.010	0.378	0.293	0.231	0.902
398	2.004	1.423	1.985	0.379	0.293	0.234	0.906
423	1.992	1.407	1.959	0.380	0.295	0.237	0.912
448	1.981	1.391	1.931	0.380	0.295	0.240	0.915
473	1.967	1.375	1.907	0.380	0.296	0.242	0.918
498	1.953	1.361	1.884	0.380	0.297	0.245	0.922
523	1.938	1.345	1.858	0.380	0.298	0.248	0.926
548	1.921	1.332	1.835	0.380	0.298	0.251	0.929
573	1.902	1.316	1.811	0.381	0.300	0.253	0.934
598	1.883	1.299	1.785	0.381	0.301	0.256	0.938
623	1.862	1.281	1.758	0.382	0.302	0.259	0.942
648	1.842	1.261	1.726	0.383	0.302	0.261	0.946
673	1.822	1.238	1.694	0.384	0.303	0.263	0.951
698	1.799	1.219	1.664	0.386	0.304	0.266	0.956
723	1.775	1.196	1.629	0.388	0.305	0.268	0.960
748	1.746	1.170	1.594	0.389	0.306	0.271	0.965
773	1.714	1.140	1.558	0.389	0.305	0.275	0.969
798	1.681	1.107	1.516	0.390	0.304	0.279	0.973
823	1.643	1.072	1.476	0.392	0.303	0.283	0.977
848	1.606	1.042	1.440	0.393	0.303	0.286	0.982
873	1.567	1.007	1.397	0.395	0.304	0.289	0.987
898	1.526	0.977	1.359	0.397	0.302	0.292	0.992
923	1.484	0.941	1.315	0.401	0.305	0.295	0.999

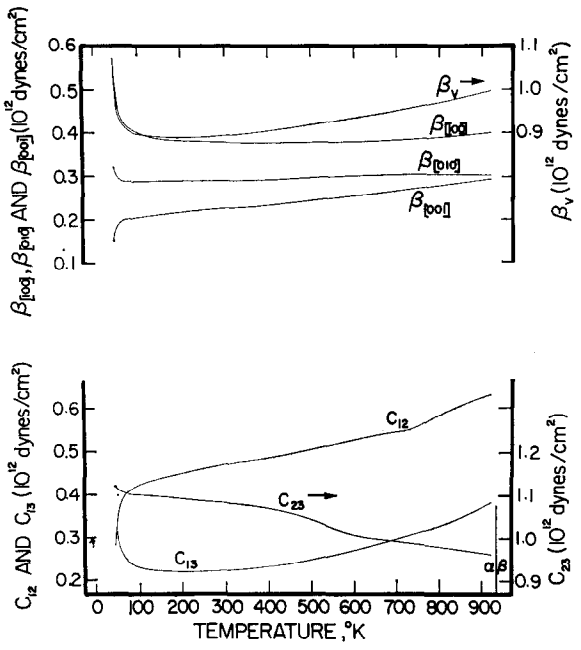

Fig. 6. Temperature dependence of the cross coupling moduli (lower half) and compressibility parameters (upper half) for alpha uranium.

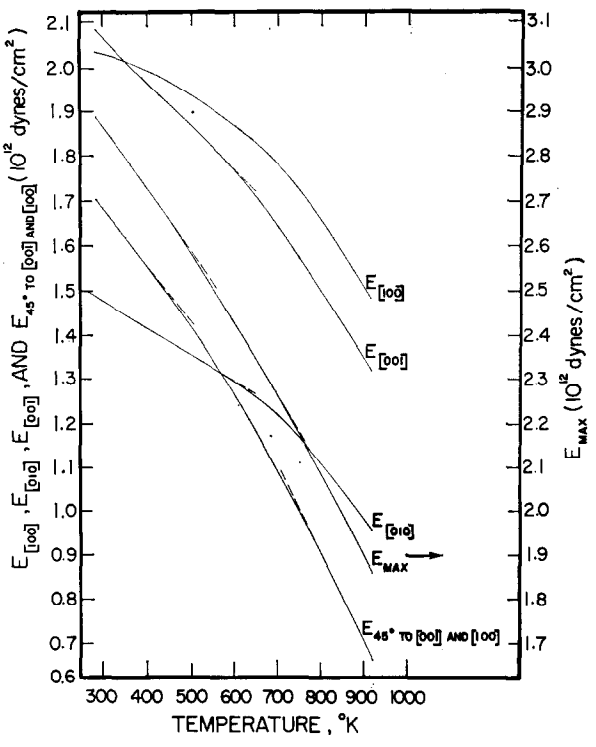

Fig. 7. Temperature dependence of the principal and the maximum and minimum Young's moduli between 300° to 923° K.

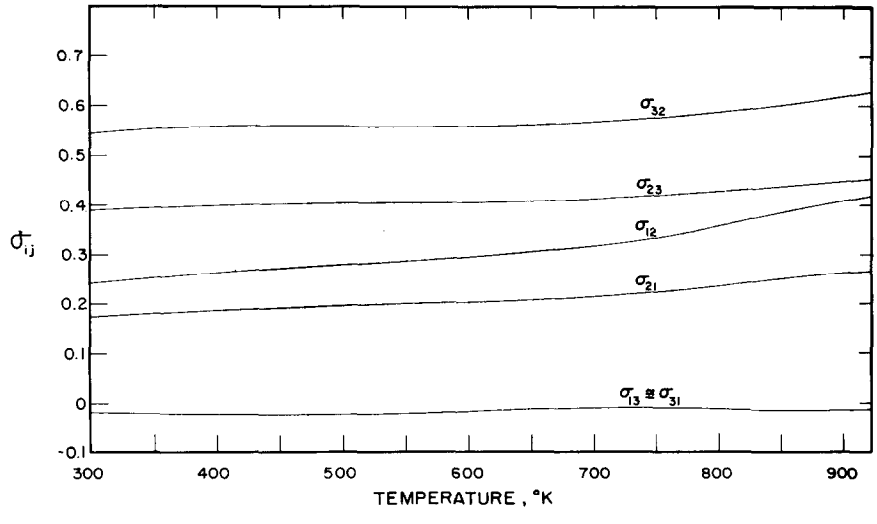

Fig. 8. Temperature dependence of the Poisson's ratio parameters between 300° and 923° K. Subscript i denotes direction of uniaxial stress and j denotes direction of coupled strain (1, 2 and 3 refer to [100], [010] and [001] directions, respectively).

The Young's moduli in the three principal directions,

$$E_{100} = 1/s_{11},\ E_{010} = 1/s_{22},\ E_{001} = 1/s_{33} \quad (3)$$

are also given in table 4 and are plotted in fig. 7 only for the 300° to 923° K range. The differences between the c_{22} and c_{33} curves and those for the corresponding E, i.e., E_{010} and E_{001} respectively, are quite pronounced, whereas, the E_{100} curve closely follows that for c_{11}. The E_{010} and E_{001} curves are, within the error of computation, straight lines in the 200° to 575° K range. Above 575° K both curves begin to decrease in slope, with very evident curvature changes.

The direction of maximum Young's modulus, E_{max}, for all temperatures above 44° K is in the (100) plane, inclined approximately 37° to the [001] direction (about 10° inclined to the nearest neighbor direction). The direction of minimum E varies with temperature, E_{010} being the smallest up to 575° K. Above 575° K the direction 45° to [001] in the (010) plane attains the minimum E value, as shown in fig. 7. The slope of the curve for the latter modulus is remarkably coincident with that for E_{max} at all temperatures above 100° K. The overall decrease from 50° to 923° K is, however, 68 % for $E_{45,}$, in contrast to 42 % for E_{max}, E_{010} and E_{001}.

The temperature dependence of the Poisson's ratios, σ_{ij}, are shown in fig. 8. The first subscript, i, denotes the direction of the unaxial stress and the second subscript, j, denotes the direction of the coupled strain, i.e. σ_{12} is the ratio of $e_{[010]}/e_{[100]}$ for $T_{[100]}$ where e and T are the directional strain and stress, respectively. These ratios are extremely anisotropic over the range of 50° to 923° K. σ_{13} and σ_{31} are very near zero throughout the temperature range, whereas the ratios that involve the [010] direction are in the range of 0.2 to 0.5 at low temperature, increase linearly with temperature between 50° and 400° K and increase with significant positive curvature above 400° K.

4. Correlation with other physical properties

The initial objectives of this study were to obtain information that would lead to an understanding of the negative linear thermal expansion coefficient, $\alpha_{[010]}$ [5]) and the anomalous specific heat at temperatures above 350° K [7]). During the course of these measurements the existence of the transition at 41° K was established, revealing several new anomalies that also require explanation. We will attempt here to associate the elastic moduli data with the anomalies in thermal expansion and specific heat and to point out a possible relationship between the low temperature and high temperature anomalies.

4.1. The thermal expansion anomalies

Between 50° K and the temperature of the $\alpha \rightarrow \beta$ phase transformation (935° K) the three linear expansion coefficients α_1, α_2 and α_3 (subscripts 1, 2 and 3 refer to the [100], [010] and [001], respectively) are all abnormally affected by temperature changes [13]). α_1 decreases with increasing temperature to a minimum in the 100° K range and then increases continuously by a factor of two between 100° and 935° K. α_2 has a small positive value at 50° K, decreases continuously to zero at approximately 350° K and has an increasingly negative temperature dependence at higher temperatures. α_3 has a very large positive temperature dependence, increasing by a factor of almost five between 50° and 923° K.

The influence of the elastic moduli on the thermal expansion coefficients can be illustrated through the Grüneisen relation:

$$\alpha_v = \frac{C_p \beta_v \Gamma_v}{V}, \quad (4)$$

where α_v is the volume expansion coefficient, C_p is the specific heat at constant pressure, V is the specific volume, β_v is the adiabatic compressibility [eq. (2)] and Γ_v is the Grüneisen coefficient, which for the present case, may arise from the changes with volume of 1. the average frequency of the normal modes of the lattice vibrations, 2. the density of electronic states of the Fermi surface and 3. the energy of magnetic interaction. These contributions are related to the total Γ_v on the basis of the weighted specific heat contributions:

$$\Gamma_v = \frac{C_g}{C_p}\Gamma_g + \frac{C_e}{C_p}\Gamma_e + \frac{C_m}{C_p}\Gamma_m \qquad (5)$$

where the subscripts g, e and m refer to the lattice, electronic and magnetic contributions respectively. In most metals Γ_g varies with temperature with values varying from 1.5 to 3. At low temperature, where C_e and C_m may be relatively large, a negative Γ_v and therefore a negative α_v may arise, as in the case of uranium below 45° K, from the Γ_e and/or Γ_m contributions. Because of the absence of compressibility values below 42° K we cannot at the present time evaluate Γ_v in this interesting temperature range. The other anomaly, α_2 above 350° K, can, however, be analyzed quantitatively using the tensor form of the Grüneisen relation to determine whether a negative Γ_v is necessarily involved in this situation [14]). The following relations are thus obtained:

$$\begin{aligned}
\frac{V}{C_p}\alpha_1 &= (s_{11}\Gamma_1 + s_{12}\Gamma_2 + s_{13}\Gamma_3) = \\
&= \frac{\Gamma_1}{E_1} - \frac{\sigma_{21}}{E_2}\Gamma_2 - \frac{\sigma_{31}}{E_3}\Gamma_3 \\
\frac{V}{C_p}\alpha_2 &= (s_{12}\Gamma_1 + s_{22}\Gamma_2 + s_{23}\Gamma_3) = \\
&= -\frac{\sigma_{12}}{E_1}\Gamma_1 + \frac{\Gamma_2}{E_2} - \frac{\sigma_{32}}{E_3}\Gamma_3 \\
\frac{V}{C_p}\alpha_3 &= (s_{13}\Gamma_1 + s_{23}\Gamma_2 + s_{33}\Gamma_3) = \\
&= -\frac{\sigma_{13}}{E_1}\Gamma_1 - \frac{\sigma_{23}}{E_2}\Gamma_2 + \frac{\Gamma_3}{E_3},
\end{aligned} \qquad (6)$$

which reduces to,

$$\alpha_v = \frac{C_p}{V}(\beta_{[100]}\Gamma_1 + \beta_{[010]}\Gamma_2 + \beta_{[001]}\Gamma_3). \qquad (7)$$

Γ_1, Γ_2 and Γ_3 are the Grüneisen coefficients which apply for uniaxial thermal strains in the [100], [010] and [001] directions respectively and the same subscript scheme applies to E_1, E_2 and E_3. The solutions for Γ_1, Γ_2, Γ_3 and Γ_v obtained from the simultaneous equations using the s_{ij} values from the present measurements, the α_i computed by Lloyd *et al.*[13]) and the total C_p[7]) are shown in the curves of fig. 9. All of the Γ_j rise quite sharply upon cooling below 100° K; Γ_v is relatively independent of temperature between 75° K and 700° K, with a value of 2.35 and decreases to 2.15 at 900° K. Γ_1 varies from 2.68 to 2.81 in this range and Γ_3 undergoes the greatest changes with limits of 2.45 and 2.97. Γ_2 is remarkably constant between 175° K and 300° K and decreases from 1.6 to 1.15 above 300° K. Although the decrease in Γ_2 may be a contributing factor, the negative α_2 arises, primarily, from the abnormally large Poisson's ratio σ_{32} and the large negative temperature dependence of E_3.

4.2. The anomalous specific heat

Fig. 10 shows the temperature dependence of various contributions to the total specific heat for alpha uranium. The C_p curve between 0° and 300° K is that given by Flotow and Lohr [15]) and the higher temperature part is due to Ginnings *et al.*[7]). The specific heat at constant volume, C_v, was derived using the thermodynamic relation

$$C_v = \left(\frac{\beta_v}{\alpha_v^2 VT + \beta_v C_p}\right) C_p^2, \qquad (8)$$

at temperature T. The lattice specific heat that was calculated from the Debye model using θ_D of 200° K [16]) is noted as the dashed line, C_D. The experimental lattice specific heat due to temperature change only, $C_v(V_0, T) - \gamma_0 T$, was computed from the C_v data by assuming a temperature independent electronic specific heat coefficient, $\gamma_0 = 26 \times 10^{-4}$ cal/mol·deg^2 [16]); and then correcting for the change in C_v with volume using the relation

$$\left(\frac{\partial C_v}{\partial V}\right)_T = T\frac{\{\beta_v(d\alpha_v/dT) - \alpha_v(d\beta_v/dT)\}}{V^2}\frac{C_v}{C_p}. \qquad (9)$$

The resulting curve approaches the C_D curve in the range of 100° to 120° K. Below 100° K the specific heat in excess of C_D increases with decreasing temperature; this reflects either a decreasing θ_D or an increasing contribution from the free electrons, or from a magnetic moment. Above 120° K the $C_v(V_0, T) - \gamma_0 T$ curve follows the Debye function reasonably well, allowing for experimental error, up to approximately 400° K where it has a significant positive curvature and increases above 3 R at higher temperatures.

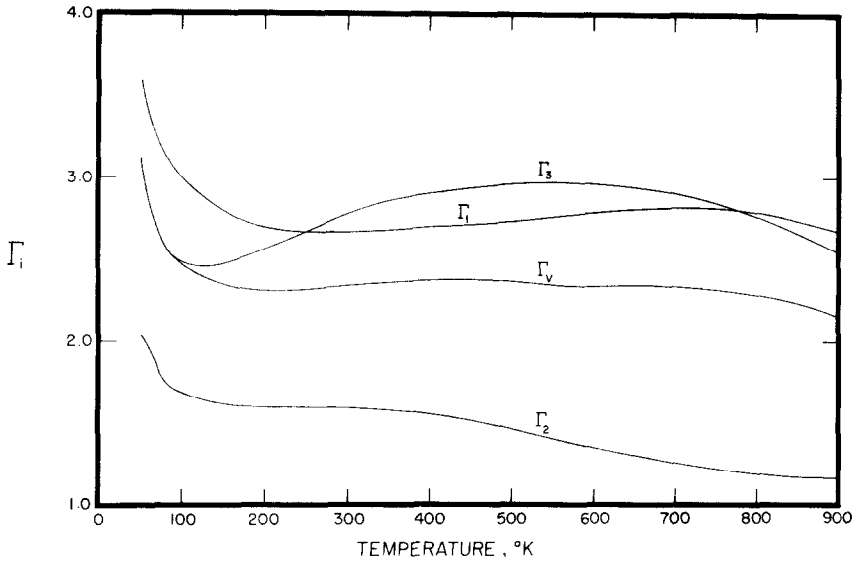

Fig. 9. The Grüneisen coefficients for principal axis strains as computed from eq. (5) of text. Γ_1, Γ_2 and Γ_3 are the coefficients due to independent strains in the principal directions and Γ_v is that arising from volume changes.

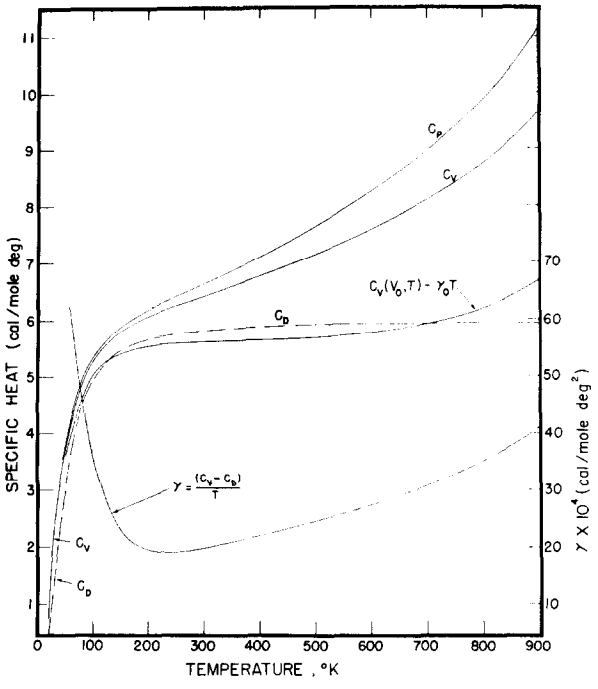

Fig. 10. Temperature dependence of C_p and C_v for uranium, from [7, 15, 16]) and lattice specific heat, $C_v(V_0, T) - \gamma_0 T$, assuming a constant electronic specific heat coefficient of 26×10^{-4} cal/deg^2·mole. C_D is the Debye function for a θ_D of 200° K (------). γ curve is electronic specific heat coefficient assuming deviation from C_D originates from electronic effects.

The temperature region where the positive curvature in the $C_v(V_0, T) - \gamma_0 T$ curve begins corresponds closely to the beginning of accelerated temperature dependence of the thermal expansion coefficients and of the c_{55} elastic modulus. This coincidence suggests that the electronic specific heat coefficient does remain temperature independent, as assumed, and that an unusually large temperature dependence of the vibrational frequency spectrum exists in the 400° to 900 °K range, which drastically reduced the effective Debye θ. This conclusion would be consistent with the measurements of the Debye-Waller temperature factor for neutron diffraction by Mueller *et al.*[17]).

There is, however, some evidence to suggest that the excess in C_v is due, at least partially, to a positive temperature dependence of the electronic specific heat coefficient, γ. The evidence, which is based on the temperature dependence of paramagnetic susceptibility, specific heat and electrical resistivity, has been reviewed by Friedel in terms of the band approximation to the electron energy states [9]). The curve marked $\gamma = (C_v - C_D)/T$ of fig. 10 represents the temperature dependence of the

electronic specific heat coefficient on the assumption that all of the deviation of C_v from C_D is due to a temperature dependent γ.

4.3. The temperature range of magnetic ordering

Although the nature of the 41° K phase transition is not yet established, it seems quite clear from the neutron diffraction evidence that some sort of superstructure of magnetic moments is involved and that the alignment of moments increases continuously upon cooling from 300° K [4]. The broad temperature range of the anomalous c_{11} temperature dependence may be interpreted as further evidence of a continuous change from a disordered to a fully ordered state. Evidently the increase in ordering below 250° K coincides with or produces a marked negative contribution to the 2nd nearest neighbor central force constant, which far exceeds the positive contribution of the decreasing temperature. Because the neutron diffraction experiments have not yet been extended to temperatures above 298° K, the temperature range in which partial magnetic ordering exists is open to question. If the unusual changes in the temperature dependence of the shear moduli and the lattice specific heat $[C_v(V_0, T) - \gamma_0 T)]$ are assumed to be the result of continuous decrease in magnetic order, it would appear that the contributions to the thermal properties begin to disappear upon heating above 400° K. It is in this range that a change in slope of the c_{55} temperature dependence occurs. From a simple central force model c_{55} is primarily associated with the long range central forces (higher than fourth nearest neighbor distances). The change in slope of the c_{66} temperature dependence in the 650° to 700° K range can in a similar manner be associated with the third nearest neighbor band. Since major changes in character of the temperature dependence of the elastic properties seem to occur in the 600° to 700° K temperature range one may conclude from these results that the magnetic ordering disappears upon heating to the range of 700° K.

The concept of a gradual increase in magnetic spin disorder with increasing temperature may also serve as an explanation for the electrical resistivity vs temperature curves which have been reported for polycrystalline uranium [36]. These data generally show a linear temperature dependence of resistivity in the 25° to 40° K range and an abrupt but small decrease in slope in the neighborhood of 40° K which is characteristic of the antiferromagnetic to paramagnetic transition in certain heavy rare earth metals. In contrast to the rare earths, $d\varrho/dT$ above the transition is only slightly smaller than that below the transition but gradually decreases with increasing temperature and the negative curvature is very pronounced above 300° K. Assuming that there are localized electron spins on the atoms, as in the case of the rare earths, the spin-disorder contribution to the electrical resistivity would increase with increasing and disorder eventually be temperatureinde pendent when the degree of order has become essentially temperature independent.

5. Conclusions

The temperature dependence of the shear moduli and the elastic parameters involving cross-coupling of strains (Young's moduli and Poisson's ratio) in alpha uranium single crystals undergo unusual changes at temperatures above 400° K, with the most significant changes occurring above 600° K. It is shown that the negative thermal expansion coefficient in the [010] direction is probably the result of the anisotropy and temperature dependence of the elastic compliance moduli. The lattice specific heat at constant volume, assuming a temperature independent electronic specific heat coefficient is shown to be relatively normal in the 100° to 400° K range, but attains a significantly positive temperature dependence above 400° K. It is suggested that the anomalies in the thermal properties and in the temperature dependence of the electrical resistivity are caused by the continuous decrease with increasing temperature of magnetic moment alignments, which are indicated by neutron diffraction measurements of Mueller [4].

Acknowledgements

This work was carried out under the auspices of the U.S. Atomic Energy Commission. Some of the measurements reviewed in this paper were carried out by Messrs. H. J. McSkimin and T. Bateman at the Bell Telephone Laboratories. Messrs. R. Black and C. J. Renken assisted in obtaining the new results given here. The author is also grateful to Drs. M. Mueller and D. Lam for helpful discussions and to Mr. L. T. Lloyd for reviewing the manuscript.

References

1) E. S. Fisher and H. J. McSkimin, J. Appl. Phys. **29** (1958) 1473
2) H. J. McSkimin and E. S. Fisher, J. Appl. Phys. **31** (1960) 1627
3) E. S. Fisher and H. J. McSkimin, Phys. Rev. **124** (1961) 67
4) C. S. Barrett, M. H. Mueller and R. L. Hitterman, Phys. Rev. **129** (1963) 625
5) J. R. Bridge, C. M. Schwartz and D. A. Vaughn, Trans. AIME **206** (1956) 1282
6) A. J. Dahl and M. S. Van Dusen, J. Res. Natl. Bur. Std. (U.S.) **39** (1947) 53
7) D. C. Ginnings and R. J. Corruccini, U.S. AEC Report NBS-A3947 (1946)
8) H. H. Chiswik *et al.*, Proc. Sec. Geneva Conf. Peaceful Uses of Atomic Energy, Vol. **6** (1958) 394
9) J. Friedel, J. Phys. Chem. Solids **1** (1956) 175
10) E. S. Fisher and C. J. Renken, Phys. Rev. **135** (1964) A482
11) H. J. McSkimin, IRE Trans. on Ultrasonic Eng. AE-5 (1957) 25
12) E. S. Fisher and C. J. Renken, J. Acoust. Soc. Am. **35** (1963) 1005
13) L. T. Lloyd and C. S. Barrett, J. Nucl. Mat. **18** (1966) 55
14) E. Grüneisen and E. Goens, Z. Phys. **29** (1924) 141
15) H. E. Flotow and H. Lohr, J. Phys. Chem. **64** (1960) 904
16) P. L. Smith and N. M. Wolcott, Conf. de Phys. des Basses Temp. (France) annexe 1955–3 (September, 1955)
17) M. H. Mueller, Argonne (USA) Report, ANL-6516 (1961) 210